PHYSICAL REVIEW D **92,** 114012 (2015)

Schottky anomaly and hadronic spectrum

Aritra Biswas,[*] M. V. N. Murthy,[†] and Nita Sinha[‡]

The Institute of Mathematical Sciences, Chennai 600113, India

(Received 1 October 2015; published 7 December 2015)

We show that the hadronic "heat capacity" calculated as a function of temperature may be used to infer the possible presence of different scales underlying the dynamical structure of hadronic resonances using the phenomenon of Schottky anomaly. We first demonstrate this possibility with the well-known meson spectrum in various channels and then comment on the possibility of using this method as a diagnostic to distinguish the exotic states.

DOI: 10.1103/PhysRevD.92.114012 PACS numbers: 14.40.-n

I. INTRODUCTION

The recent announcement of the discovery[1] of the so-called pentaquark states has rekindled interest in the possibility of exotic hadron states. In the last decade, a large number of exotic mesonic states known as the X, Y, Z states [2] has been observed by different experimental collaborations (BELLE, *BABAR*, BESIII, CDF, CLEO, LHCb, etc.) [3]. Long ago, a proposal was made to identify the $\Lambda(1405)$ baryon as a possible molecular state of a colorless baryon and meson [4–6]. Recently this proposal was confirmed through lattice calculations [7].

While the existence of such exotic states has been theoretically studied over decades [8–13] using models of quark confinement with hyperfine interaction, we explore the possibility of identifying states which differ in their underlying dynamics due to different interaction scales responsible for forming composite states such as mesons. This is a model-independent analysis which depends entirely on the information already contained in the experimental data on the spectra of composite states.

The method itself is not new. It has been in vogue in the study of semiconductors with impurities (which may have closely spaced electronic spectra) or in the analysis of spectra of deformed nuclear states for a long time. In principle when the number of states is large, the high temperature behavior of the specific heat directly yields the information about the relevant degrees of freedom in the spectrum—this is the well-known Dulong-Petit law. This has been effectively put to use in the analysis of the light baryon spectrum by Bhaduri and Dey [14] where they have shown that even with the truncated spectrum of light quark baryon states, the degrees of freedom of the system may be inferred by comparing the models with the experimental spectrum through the so-called Schottky peak. However, such an analysis cannot be applied to the meson spectrum to infer the degrees of freedom as may be inferred from an analysis of the meson spectrum.

On the other hand, when a truncated spectrum is available with no saturation possible, the specific heat at low temperature displays a Schottky peak (or peaks) which is an indication of the relevant scale (scales) in the system. Therefore the method we use here consists of analyzing the heat capacity C_V of a spectrum of states which may contain finitely many states that may not lead to saturation of the specific heat. The existence of the Schottky peak (peaks) is taken as an indication of the presence of an interaction scale (scales) and analyzed further. This provides a possible model-independent diagnostic of the presence of unusual or exotic states. The only input used is the experimentally measured spectrum of states.

In Sec. II, we illustrate the method with a set of assumed ideal spectra closely following the illustrations adopted from Ref. [15]. Though the method has been widely used in other fields, it may not be familiar to the practitioners in particle physics phenomenology. In Sec. III we first discuss the charmonium spectrum to illustrate the applicability of the method to the measured spectrum of states using the lists provided in PDG [16]. The charmonium spectrum provides a template for the analysis of other states. Further, we discuss other cases, including the bottomonium and open-charm/bottom mesons, and show that interesting facts emerge by a simple application of the idea of the Schottky anomaly. We conclude with a mention of caveats and how the method may be fruitfully used as and when more data become available, particularly for the conjectured exotic bottomonium states.

II. HEAT CAPACITY OF AN IDEAL SYSTEM

In order to illustrate the method, consider the simplest case of a two-level system with an energy gap given by Δ. The energy gap is an indication of the scale in the Hamiltonian. The canonical partition function of the system is simply given by

$$Z = 1 + e^{-\beta\Delta}, \tag{1}$$

[*]aritrab@imsc.res.in
[†]murthy@imsc.res.in
[‡]nita@imsc.res.in

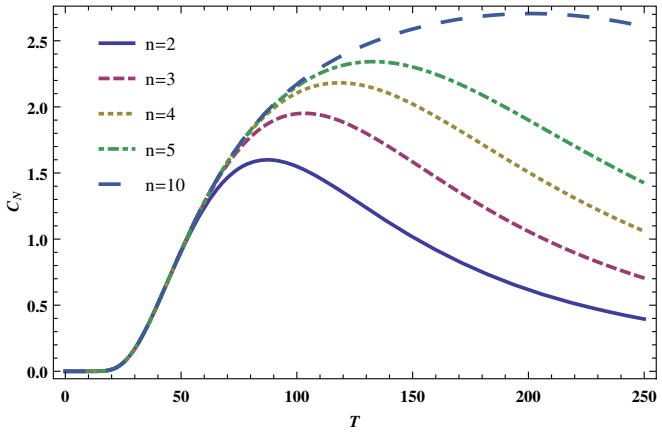

FIG. 1 (color online). Schematic illustration of the Schottky peak in the three-dimensional harmonic oscillator spectrum showing the effect of truncation of the spectrum.

where $\beta = 1/k_B T$ is the inverse temperature. Hereafter we set the Boltzmann constant $k_B = 1$ and the temperature is given in energy units. For the purpose of illustration here we have not assumed any occupancy factors. The temperature is introduced here simply as a mathematical parameter to define the partition function of the system and no assumption is made regarding the system being in a heat bath in equilibrium. It is a parameter that is used to calculate the specific heat or more precisely energy fluctuations.

The specific heat of the system at constant volume may be defined as

$$C_V = \beta^2 \left[\frac{1}{Z} \frac{\partial^2 Z}{\partial \beta^2} - \left(\frac{1}{Z} \frac{\partial Z}{\partial \beta} \right)^2 \right] = \beta^2 [\langle E^2 \rangle - \langle E \rangle^2]. \quad (2)$$

In systems with constant density, we may replace C_V by C_V. Substituting for the partition function of the two-level system given in Eq. (1) we have

$$C_V = \beta^2 \frac{\Delta^2 e^{-\beta\Delta}}{(1 + e^{-\beta\Delta})^2}. \quad (3)$$

When C_V is plotted against $\beta\Delta$ the Schottky peak appears at a value $\beta\Delta \approx 2.4$ with an exponential tail at higher values of β. The location of the peak is a function of the energy gap in the system. In general the Schottky peak occurs in

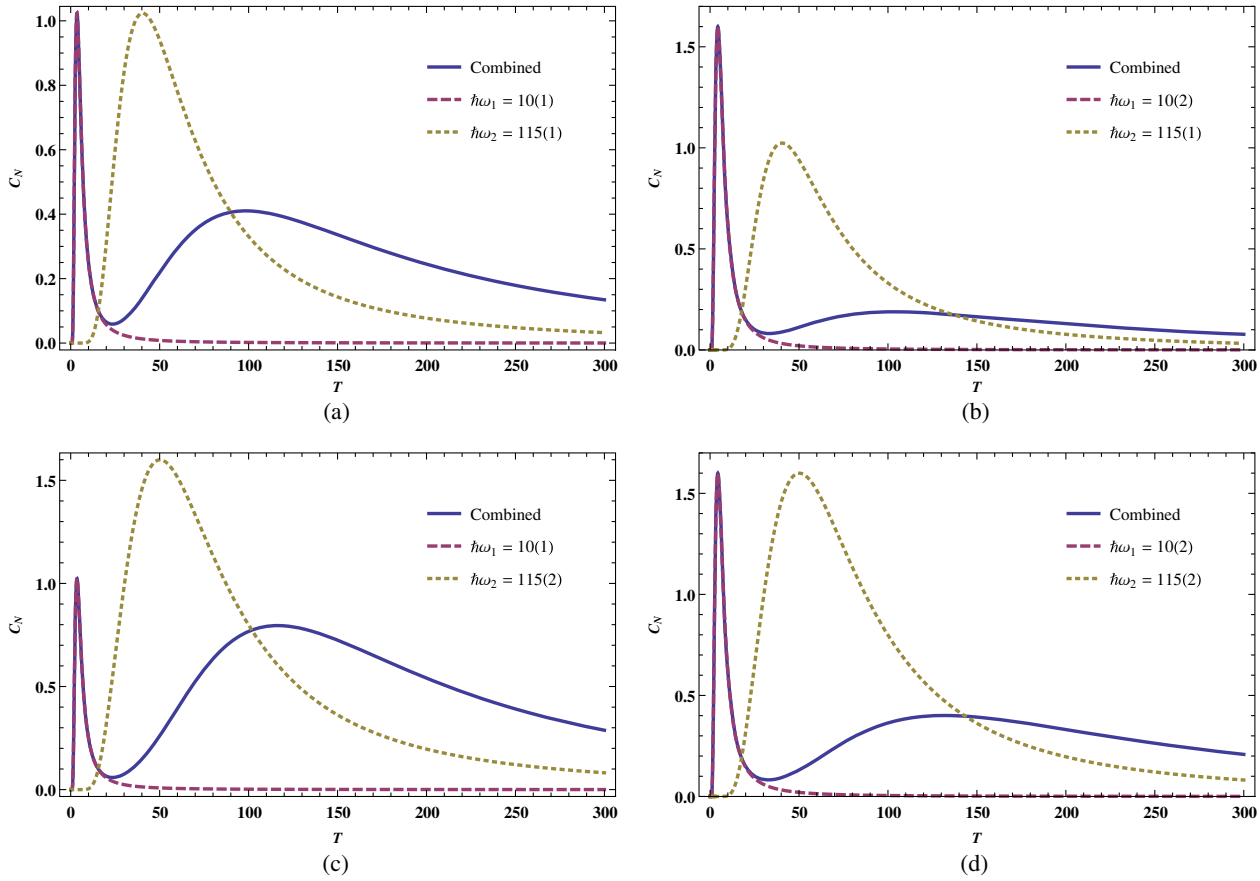

FIG. 2 (color online). Schematic illustration of the Schottky peaks in the ideal case when the data contain two scales. The individual Schottky peaks corresponding to separate spectra (harmonic oscillator spectrum), as well as the combined one (solid line), are shown. The frequencies are the same for all four figures as shown ($\hbar\omega_1 = 10$ MeV and $\hbar\omega_2 = 115$ MeV). The cutoffs in the principle quantum number n (indicated in brackets) are (a) $n_1 = n_2 = 1$, (b) $n_1 = 2$ $n_2 = 1$, (c) $n_1 = 1$ $n_2 = 2$, and (d) $n_1 = n_2 = 2$.

TABLE I. Charmonium masses given in MeV along with their total angular momentum J. Other quantum numbers are not needed for this analysis.

$J=0$ states	Mass (MeV)	$J=1$ states	Mass (MeV)	$J=2$ states	Mass (MeV)
$\eta_c(1S)$	2983.6	$J/\psi(1S)$	3096.92	$\chi_{c2}(1P)$	3556.2
$\chi_{c0}(1P)$	3414.75	$\chi_{c1}(1P)$	3510.66	$\chi_{c2}(2P)$	3927.2
$\eta_c(2S)$	3639.4	$h_c(1P)$	3525.38		
$\chi_{c0}(2P)$	3918.4	$\psi(2S)$	3686.11		
		$\psi(3770)$	3773.15		
		$\psi(4040)$	4039.6		
		$\psi(4160)$	4191		
		$\psi(4415)$	4421		

systems with few energy levels where gaps are a result of a single scale parameter. If, however, there is more than one independent scale parameter responsible for the energy levels, then peaks appear whenever the temperature is sufficient to cross the gap signaling a change in the entropy of the system. At high temperatures when all the levels are equally possible, a plateau appears, signaling very little change in the entropy.

To further expand on this theme, we next consider an ideal spectrum, namely, the spectrum of a three-dimensional harmonic oscillator. The partition function of the system is given by

$$Z_1 = \sum_{n=0}^{\infty} D(n) e^{-\beta\hbar\omega(n+3/2)}, \tag{4}$$

where the oscillator parameter ω defines the scale in the problem and $D(n)$ is the degeneracy of the level. In Fig. 1, we show the effect of truncation on the specific heat when plotted as a function of $T = 1/\beta$ with $\hbar\omega = 200$ MeV (for example). As we include more and more orbitals, the specific heat tends to reach the required saturation, while the peak persists in the truncated spectrum. As we shall see later, in any realistic hadronic spectrum, especially in the heavy quark sector, we do not need more than two to three orbitals to count the observed spectrum of states. For these cases the location of the Schottky peak is close to $\beta\hbar\omega \approx 2.42$.

In order to simulate realistic spectra where there is a possibility of more than one energy scale in operation, we combine the spectra of two such systems which differ in $\hbar\omega$ significantly. In Fig. 2 we show the individual spectra separately as well as the spectra for the combined single set. The effect of combining is to normalize the specific heat with a single partition function given by

$$Z(\beta) = Z_1(\beta, \hbar\omega_1) + Z_2(\beta, \hbar\omega_2). \tag{5}$$

This is somewhat artificial but nevertheless we use this for the purpose of illustrating the effect of the presence of multiple scales in the spectra when the states are combined in a listing in the absence of any dynamical information.

As can be seen from Fig. 2 the amplitude and location of the two separate Schottky peaks depend on truncation apart from the oscillator frequencies. When combined, the peak corresponding to the lower frequency remains unchanged while the one corresponding to the higher frequency is sensitive to truncation. This is simply due to the domination of the lower scale in the partition function.

We exploit this sensitivity to different scales in the problem, and apply it in the analysis of experimental spectra of sets of mesons in the next section. Different scales may arise from different terms in the same Hamiltonian; for example, the confinement scale could be very different from the splitting of states with different spins, namely, the hyperfine splitting. Alternatively the data set could contain states which may arise from different underlying dynamics and hence have different scales. Often it may so happen that the data set is missing a certain

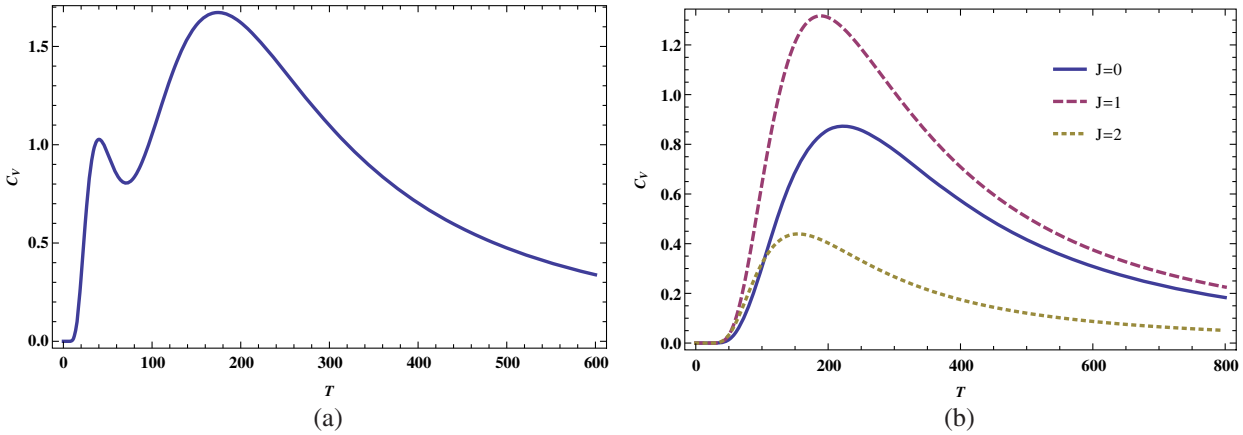

FIG. 3 (color online). The specific heat of charmonium states plotted as a function of temperature (expressed in MeV units) with (a) all the states taken together (i.e., all the states in Table I) and (b) after separating them according to their spins $J = 0$, 1, 2 (columns 3, 6, and 9 of Table I).

TABLE II. The exotics in the charmonium mass range. All masses except that of $Y(4008)$ are taken from PDG [16]. The mass of $Y(4008)$, as well as some of the J assignments not given in PDG, is from [2].

$J=0$ states	Mass (MeV)	$J=1$ states	Mass (MeV)
$X(3940)$ [17]	3942	$X(3872)$ [18,19]	3871.69
$Y(4140)$ [20]	4144	$X(3900)$ [21]	3896.35
$X(4160)$ [22]	4156	$X(4260)$ [23,24]	4251
		$Y(4360)$ [25]	4361
		$X(4430)^{\pm}$ [26]	4485
		$X(4660)$ [27]	4664
		$Y(4008)$ [23]	4008
		$Z_c^+(4020)$ [28]	4024
		$Z_1^+(4050)$ [29]	4051
		$Z^+(4200)$ [30]	4196
		$Z_2^+(4250)$ [29]	4248
		$X(4630)$ [31]	4634

number of states, which also introduces an artificial scale (or energy gap) in the analysis. Nevertheless, the analysis of Schottky peaks in the experimental spectra may reveal some hidden scales on the average. We must however caution that this analysis will not reveal any detailed dynamics (or the system Hamiltonian) underlying the formation of the bound states.

III. ANALYSIS OF THE EXPERIMENTAL DATA

We consider an analysis, based on the template given in the previous section, of the experimental data on mesons. We divide the data sets according to their flavors and start from the simplest cases, where there is no complication arising from the isospin degeneracies. In this analysis we only use the identification given in the particle data group tables without any further theoretical bias. We focus on the heavy quark sector.

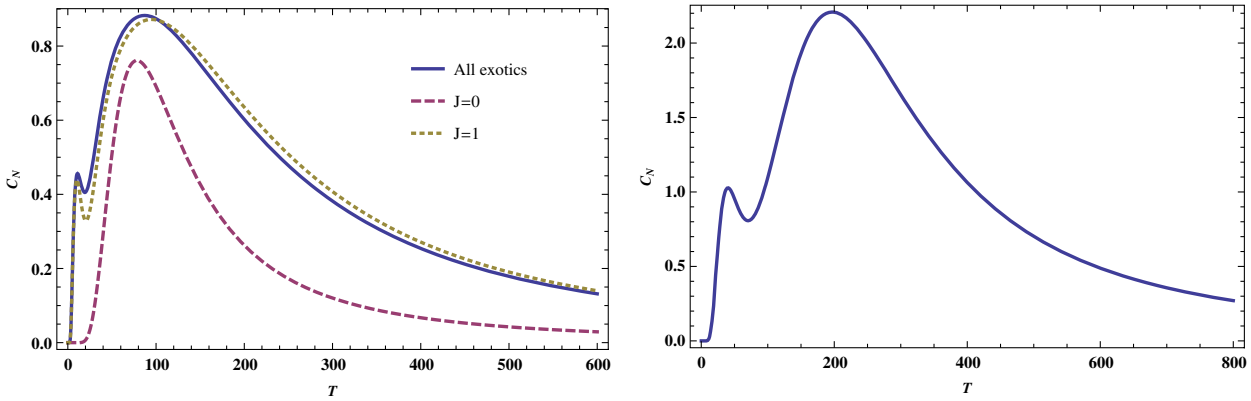

FIG. 4 (color online). The specific heat of the exotics as listed in [2,16] in the charmonium region, plotted as a function of temperature (a) for the pure exotics spectrum (i.e., states from Table II) and the same separated according to the corresponding J's only and (b) combined with all the other $c\bar{c}$ states (i.e., all states from Tables I and II combined).

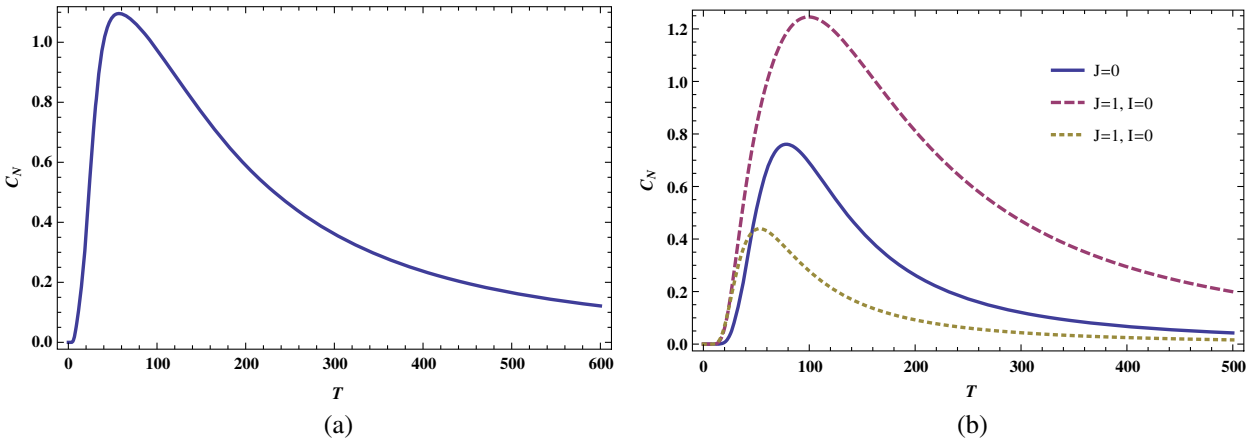

FIG. 5 (color online). (a) The single peak obtained by omitting the resonance at 3872 MeV from the other exotics. (b) The exotics plotted after the assignment of the I values, separated into corresponding groups with the same J and I.

TABLE III. Bottomonium masses given in MeV along with their total J. Other quantum numbers are not needed for this analysis.

$J=0$ states	Mass (MeV)	$J=1$ states	Mass (MeV)	$J=2$ states	Mass (MeV)
$\eta_b(1S)$	9398	$\Upsilon(1S)$	9460.3	$\chi_{b2}(1P)$	9912.21
$\chi_{b0}(1P)$	9859.44	$\chi_{b1}(1P)$	9892.78	$\Upsilon(1D)$	10163.7
$\eta_b(2S)$	9999	$h_b(1P)$	9899.3	$\chi_{b2}(2P)$	10268.7
$\chi_{b0}(2P)$	10232.5	$\Upsilon(2S)$	10023.3		
		$\chi_{b1}(2P)$	10255.5		
		$h_b(2P)$	10259.8		
		$\Upsilon(3S)$	10355.2		
		$\Upsilon(4S)$	10579.4		
		$\Upsilon(10860)$	10876		
		$\Upsilon(11020)$	11019		

A. The spectra of charmonium states

We first choose to analyze the spectra of the $c\bar{c}$ (charmonium) states as identified in the PDG [16], listed in Table I. Since the number of resonant states is not too small (but nowhere near saturation), the spectra may be used to determine the scales involved in the problem. Since these states involve heavy quarks, one may also compare the results of the analysis with models of confinement if necessary. In Fig. 3(a) we show the specific heat of the $c\bar{c}$ spectrum.

When all the $c\bar{c}$ are taken together, the spectrum shows two clear peaks at $T \approx 40$ MeV and $T \approx 190$ MeV, indicating the existence of two well-defined scales in the spectrum of states. This is not surprising since all of the states with different J values, $J = 0, 1, 2$, are included. As a result not only the confinement scale, but also the hyperfine (HF) splitting scale comes into operation. We may think of the peak at 40 MeV as being due to the HF splitting, whereas the peak at 190 MeV results from the confinement scale. For a two-level system, using the relation $\beta\Delta = 2.4$, the corresponding energy gap turns out to be 96 MeV for hyperfine splitting and 450 MeV for the confinement potential. These are reasonable values from the point of view of quark models though we need not assume any particular model for the charmonium states. These scales reflect the average behavior, since the actual value of

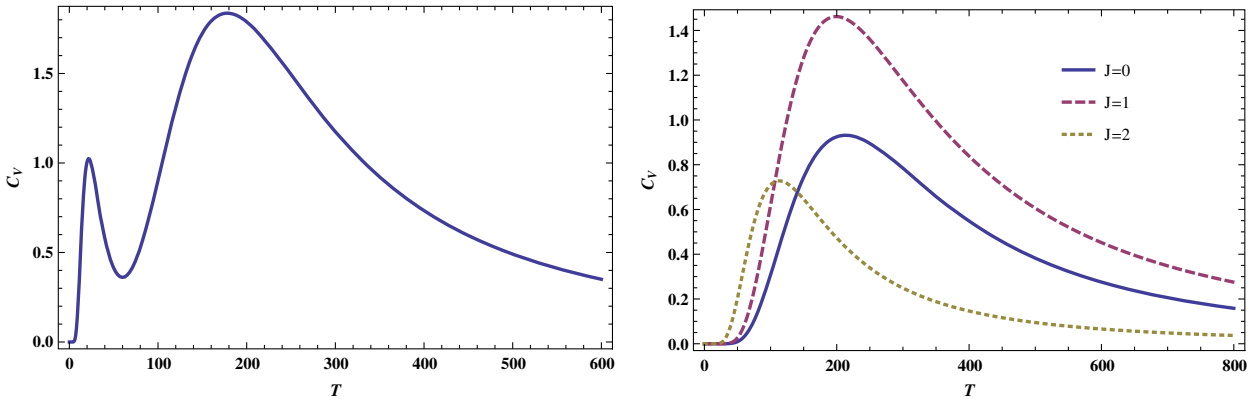

(a) (b)

FIG. 6 (color online). The specific heat of bottomonium states plotted as a function of temperature (expressed in MeV units) (a) with all the states in Table III and (b) after separating them according to their spins $J = 0, 1, 2$.

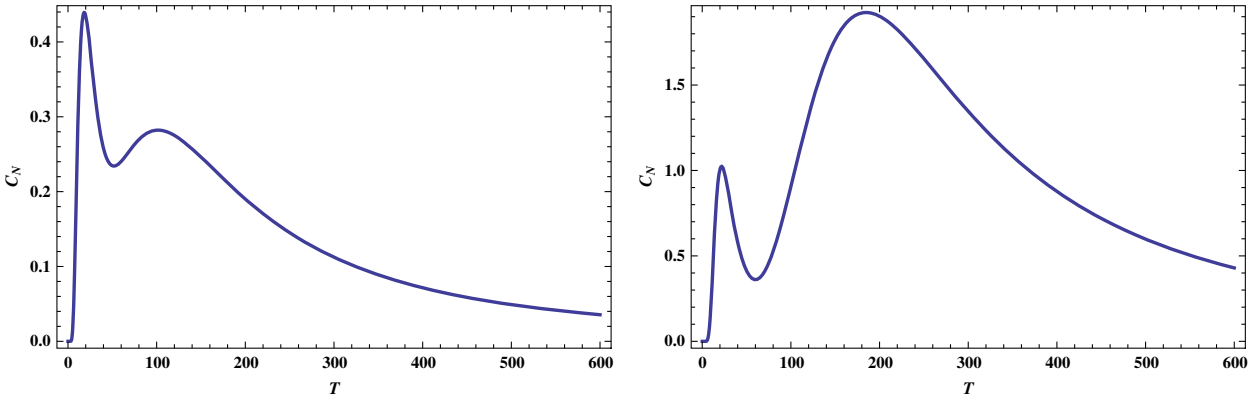

(a) (b)

FIG. 7 (color online). The specific heat of the exotics as listed in PDG in the bottomonium mass range (a) with only the exotic states and (b) combined with pure bottomonium states (i.e., combined with all the states of Table III).

TABLE IV. Masses of open charm mesons given in MeV along with their total J and I.

$J=0$ states	I	Mass (MeV)	$J=1$ states	I	Mass (MeV)	$J=2$ states	I	Mass (MeV)
$D_s^{\pm}$	0	1968.30	$D_{s1}(2460)^{\pm}$	0	2459.5	$D_2^*(2460)$	$\frac{1}{2}$	2463.453
$D_{s0}^*(2317)^{\pm}$	0	2317.7	$D_{s1}(2536)^{\pm}$	0	2535.10			
D	$\frac{1}{2}$	1867.225	$D_{s1}^*(2700)^{\pm}$	0	2709			
$D_0^*(2400)^0$	$\frac{1}{2}$	2318	$D^*(2007)$	$\frac{1}{2}$	2008.61			
$D_0^*(2400)^{\pm}$	$\frac{1}{2}$	2403	$D_1(2420)$	$\frac{1}{2}$	2422.3			
$D_1(2420)^{\pm}$	$\frac{1}{2}$	2539.4	$D_1(2430)^0$	$\frac{1}{2}$	2427			

HF splitting depends on the orbital in which it is calculated. For example, in the ground state the HF splitting is of the order of 100 MeV.

These two scales must correspond to the contribution to the masses of the resonances from the QCD-inspired potential models (or in lattice calculations), where the central potential is assumed to be a combination of the linear confinement potential and the Coulomb-like potential arising from one-gluon exchange interaction,

$$V(r) = Cr + \frac{4\alpha_s}{3r}, \tag{6}$$

while the hyperfine interaction, which also arises along with the Coulomb interaction from the one-gluon exchange interaction, in general has the form

$$V_{hf}(r) = k\frac{\sigma_1.\sigma_2}{m_1 m_2} f(r). \tag{7}$$

Such a nonrelativistic reduction of the QCD-inspired potential is a good approximation in the heavy quark sector. In this paper we do not go into the details of the models but give these here only to indicate possible origins of the Schottky peaks. It is sufficient to point out that the central potential, which is spin and flavor independent, contributes in all sectors, while the HF splitting depends inversely on the quark masses as well as the particular orbital in which the spin-dependent potential is evaluated.

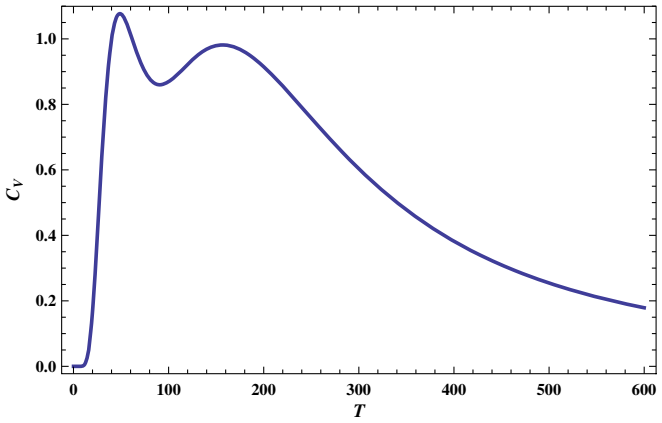

FIG. 8 (color online). C_v vs T plot for open charm mesons with all the states in Table IV.

To clarify this notion further, in Fig. 3(b) we plot the states corresponding to different J values separately. It is easily seen that the peak corresponding to HF splitting disappears as it should when different J states are plotted separately. As a result there is only one scale in the problem due to the central potential. The slight shift in the peaks in the specific heat is due to the effect of truncation of the states as noticed in the ideal case in the previous section. While there are more states in $J=0$, 1, there are only two states in the case of $J=2$. In either case, the number of orbitals involved will not be more than two to three even if a model is invoked.

Thus, having understood the charmonium spectrum where the two scales, confinement, and HF interaction energies stand out, we may now apply the method to the so-called exotic states listed along with the charmonium states. Table II shows the states used in the present analysis. Some of these assignments may be tentative or educated guesses as discussed in [2]. Nevertheless the specific heat of these states may be calculated and is shown in Fig. 4(a).

The specific heat plot shows two peaks, one reasonably broad peak close to 100 MeV and a very sharp one below 10 MeV. The peak at 100 MeV is a unique characteristic of only the exotics. For a two-level system, using $\beta\Delta = 2.4$, the corresponding energy gap is found to be 240 MeV in contrast to the pure $c\bar{c}$ case, where it is close to 450 MeV, and can be attributed to the confinement scale. The "confinement peak" is also present in the combined plots for the charmonium states along with the exotics [Fig. 4(b)], but not for the exotics alone. This indicates the presence of a scale that is different from the confinement, hyperfine, or any other scale that is exhibited by the established charmonium states. This definitely hints at a different interaction mechanism for formation of the exotic meson states. This may be called the "exotic" scale, as in the next section we show that this same scale is present for the exotics in the bottomonium mass range as well.

It is easily seen that the sharp peak below 10 MeV arises due to contributions from the first two states, which are indeed very close in energy. Since the mass of $X(3872)$ is very close to the $D^0\bar{D}^{*0}$ threshold, it was described in many reports earlier as a molecular state [32–36]. However, the characteristics of $X(3872)$ production in high energy $p\bar{p}$ and pp collisions, as reported by LHCb [19] and CMS [37]

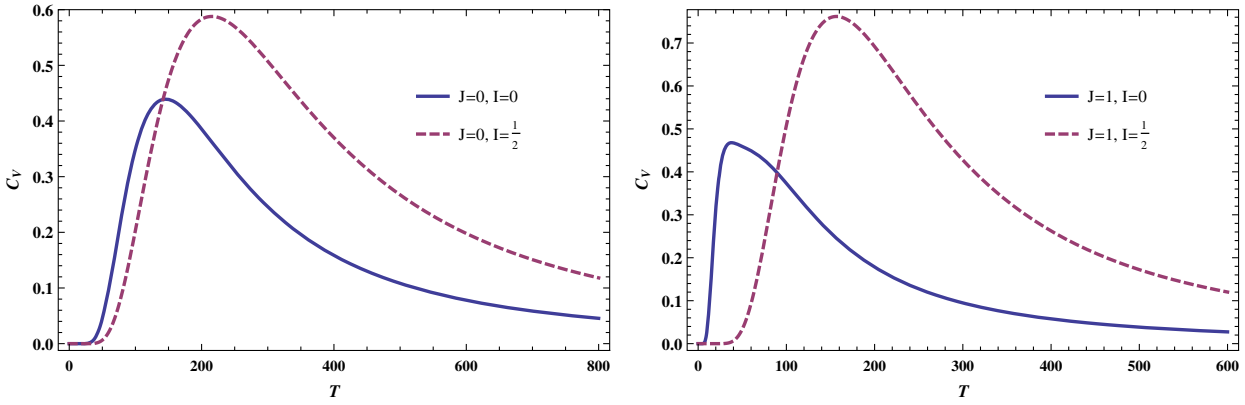

FIG. 9 (color online). C_v vs T plot for open charm mesons (a) with $J = 0$ states (column 3 of Table IV) and (b) with $J = 1$ states (column 6 of Table IV) separated according to the I values.

and discussed in [38], match those of a tightly bound state, rather than that of a molecule. If this lowest state is removed from the list of exotics it is seen that the sharp peak below 10 MeV disappears, leaving a single peak close to 60 MeV as shown in Fig. 5(a). The nature of the state at 3872 MeV cannot be inferred from the present analysis. The appearance of more such states, if at all, is needed to clarify its nature. Nevertheless if it is included in the present set, it possibly indicates the existence of states with much weaker interaction.

There can be a second explanation for the sharp peak below 10 MeV. The 3896.35 and the 4024 MeV states have been claimed to be isospin triplets, but this is not yet confirmed. Assuming them to be isospin triplets, and hence taking care of the I symmetry along with the J symmetry (by assuming others to be $I = 0$), the plots immediately exhibit the absence of the said peak, even though the 3872 resonance is included in the $J = 1, I = 0$ set [see Fig. 5(b)]. The peaks are close to $T = 100$ ($J = 0$); $T = 80$ ($J = 1$, $I = 0$); and $T = 50$ ($J = 1$, $I = 1$) in MeV units. These differences may be due to a combination of isospin symmetry breaking as well as truncation effects.

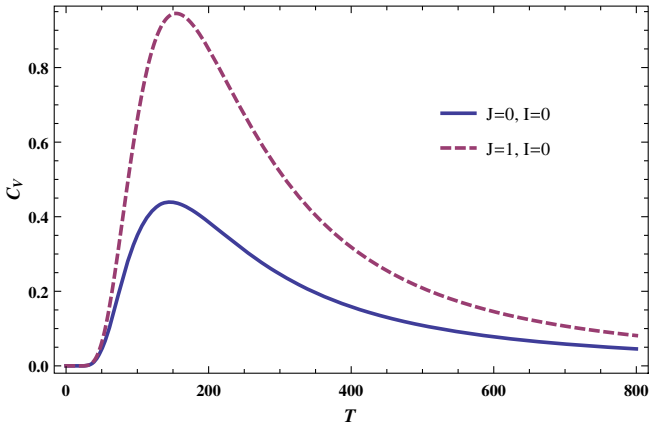

FIG. 10 (color online). C_v vs T plot for $I = 0$ states grouped into $J = 0$ and $J = 1$ after assigning $J = 1$ to $D_s^{*\pm}$ with mass 2112.1 MeV.

B. The spectra of bottomonium states

Encouraged by the considerations in the charmonium spectrum, we now analyze the bottomonium spectrum, which includes the states given in Table III. Here there are fewer observed states.

When the specific heats corresponding to these states are calculated and plotted together, the situation is quite similar to that of the charmonium states. One observes two clear peaks close to $T = 185$ MeV and $T = 22$ MeV as seen in Fig. 6(a). The peak at lower T disappears when the states are separated into groups with the same J value and plotted again [Fig. 6(b)]. This shows that the peak at lower T corresponds to the HF splitting and is thus absent when the states are separated according to spin, while that at higher T reflects the confinement scale and hence it remains even in Fig. 6(b). The peak for the $J = 2$ states is at a slightly lesser T value, but then, there are just three corresponding states. With more bottomonium states in the $J = 2$ sector, we expect the peak to shift to the right and come close to the $T = 185$ MeV value. Interestingly the HF peak in Fig. 6(a) occurs at a reduced temperature as it should, but it does not scale with the masses in accordance with Eq. (7). The difference may be an effect arising from the matrix elements. In the s-state, this may be approximated by $|\psi_s(0)|^2$. It is therefore possible that the bottomonium wave functions are more sharply peaked compared to the charmonium states.

Next, we repeat the analysis with the so-called exotics listed by PDG in the bottomonium mass range. The states are $Y_b(10890)$ [39], $X(10650)^{\pm}$ [40], and $X(10610)$ [40,41] with masses 10888.4, 10652.2, and 10608.1, respectively (all in MeV). All of them have $J = 1$ and $I = 1$. When plotted against temperature, they again exhibit two well-defined peaks at approximately $T = 19$ and

TABLE V. Masses of open bottom mesons given in MeV along with their total J and I.

$J=0$ states	I	Mass (MeV)	$J=1$ states	I	Mass (MeV)	$J=2$ states	I	Mass (MeV)
B_s^0	0	5366.77	B_s^*	0	5415.4	$B_{s2}^*(5830)^0$	0	5839.96
$B_c^\pm$	0	6275.6	$B_{s1}(5830)^0$	0	5828.7	$B_2^*(5747)^0$	$\frac{1}{2}$	5743
B	$\frac{1}{2}$	5279.42	B^*	$\frac{1}{2}$	5325.2			
			$B_1(5721)^0$	$\frac{1}{2}$	5723.5			

$T = 101$ MeV [Fig. 7(a)]. Since the quantum numbers of these states are not well defined, it is difficult to comment on these scales. However, similar to the charmonium exotics, the exotic peak close to 100 MeV is present for the bottomonium exotics also, even with as few as three states. This leads to the important conclusion that the underlying mechanism may be similar for both the charmonium and bottomonium exotics. The validity of this claim can be tested in the future with the advent of more data, especially in the bottomonium sector.

Similar to their charmonium counterpart, when the exotics are combined together with established bottomonium states and plotted, the spectra are almost similar to that of pure bottomonium states displaying a peak corresponding to the hyperfine splitting and another close to $T = 200$ MeV corresponding to the confinement scale [Fig. 7(b)].

C. The spectra of open charm states

In the previous two subsections, we have analyzed the heavy quarkonium spectra. Using the location of the Schottky peaks, we may identify, using the intuition from the potential models, the average energy scales corresponding to the central and HF interactions. The main advantage here is that there is no complication arising from isospin assignments since $I = 0$ unless they are exotic states. This simplicity is lost when we consider states which have one or more light quarks. Nevertheless, we may look at the data in this sector to gain further insights. In this subsection we look at the data on the specific heat in the open charm sector. The data used in the analysis are given in Table IV.

Figure 8 shows the specific heat calculated using all the states in the open charm spectrum plotted as a function of T. We see two peaks at temperatures close to $T = 50$ and $T = 160$ in MeV units. As usual the peak at higher T represents the flavor-independent part of the potential. The scale of HF interactions is larger than it should be since the splitting involves a light and a heavy quark.

We may analyze the data further by separating them according to the spins. The $J = 2$ sector cannot display any Schottky peak since it only has one state with $I = \frac{1}{2}$ and none with $I = 0$. In Fig. 9(a) we show the $J = 0$ spectra. The two peaks above 150 MeV correspond to isospins $I = 0$ and $I = 1/2$. In the latter case the peak shifts to the right since there are more states as seen in the effect of truncation in the ideal case discussed in Sec. II. The $J = 1$ sector is shown in Fig. 9(b) where again we have shown the $I = 0$ and $I = 1/2$ cases separately. In the $I = 1/2$ case, one may clearly see the usual confinement peak close to $T = 160$ MeV. The $I = 0$ plot indicates a single peak with a shoulder at 40 MeV.

PDG includes $D_s^{*\pm}$ with mass 2112.1 with $I = 0$, but states that its J is unmeasured. However, the corresponding decay modes of this state are consistent with $J = 1$. Including this state in the $J = 1$, $I = 0$ set immediately brings the corresponding peak to approximately the same position as the $J = 0$, $I = 0$ peak (Fig. 10). Hence, this confirms that this state actually is indeed a J triplet.

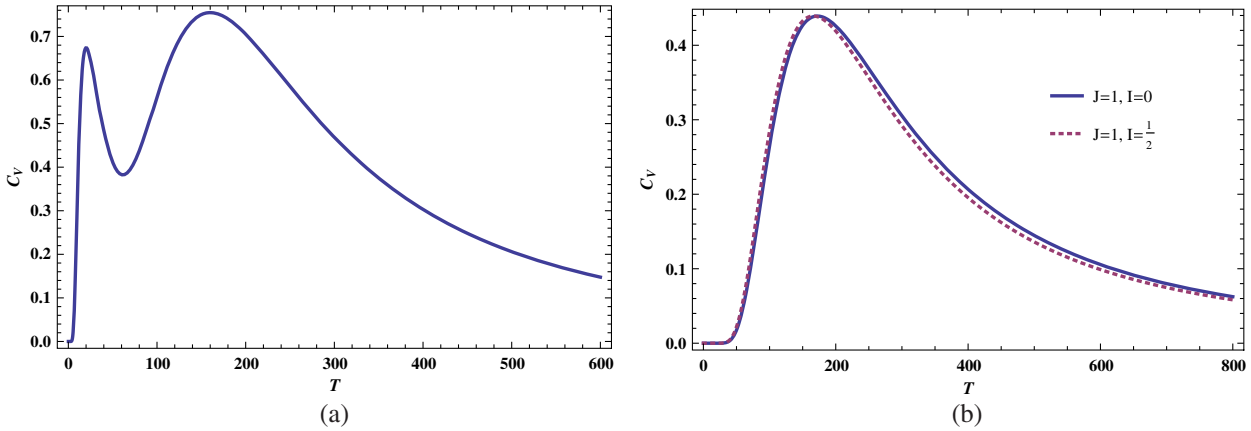

FIG. 11 (color online). C_v vs T plot for open bottom mesons (a) with all the states given in Table V and (b) with $J = 1$ states (column 6 of Table V) grouped according to the I values.

D. The spectra of open bottom states

Unlike the open charm spectra, the spectra of open bottom states are even more sparse as shown in Table V.

Nevertheless some features are already visible. For example, when all the states are plotted together as shown in Fig. 11(a), we discern the confinement as well as the HF peak (at a reduced temperature), similar to the open charm scenario.

Separation into various J and I lists cannot be carried out here since there are only two states each in the $J = 0$, $I = 0$; $J = 1$, $I = 0$; and $J = 1$, $I = \frac{1}{2}$ sectors. It is not possible to plot the $J = 0$, $I = 0$ states against T due to different flavor contents. For example, the 5366.77 MeV state is a B_s (b and s quark) state whereas the 6275.6 MeV state is a B_c (b and c quark) state.

For completeness, we may however plot the $J = 1, I = 0$ and $J = 1, I = \frac{1}{2}$ states, each of which has only two states. We show the plot in Fig. 11(b), where again the peaks coincide, indicating the confinement scale. More detailed analysis must wait for more data.

IV. SUMMARY AND CONCLUSIONS

We have presented a model-independent analysis of the data on the meson spectra using the Schottky anomaly. Given a spectrum of states, the specific heat (or equivalently energy fluctuation) when plotted as a function of temperature displays peaks, known as Schottky peaks, corresponding to the different scales present in the interaction Hamiltonian which gives rise to such states. The peaks are well pronounced, especially if the spectrum is truncated with very few orbitals as in the case of meson spectra. The corresponding temperature at which the Schottky peaks occur may be converted into energy scales relevant to the spectra on hand. This method is well known in other areas of physics.

In this analysis temperature is simply treated as a parameter which is used to extract the scale and should not be confused with the thermodynamic temperature. The information so obtained is nothing new since it is already contained in the spectra, but it provides a new way of looking at the data and analyzing the same. This is especially useful if a given set of states, in the absence of any other information, contains states which may have their origin in different types of interaction Hamiltonians, for example, the presence of exotics in the quarkonium states. Unlike the models of quarkonium states, no dynamical information may be extracted. But the intuition from the potential models or lattice calculations may be used to gain more insight.

After explaining the salient features of the method through an ideal case, we have analyzed the experimental data as listed in the latest edition of PDG. In summary we have

(i) The simplest to analyze are the quarkonium states, especially the charmonium states. Using this as a template we show how the two main scales corresponding to flavor-independent confinement interaction and the HF interaction may be seen from the representation of the data through Schottky peaks. Typically the average confinement scale (corresponding to the radial potential in a model) results in a peak around $T = 200$ MeV. If we are to interpret this information in terms of the actual scale of confinement, we need to invoke a model. If there are only two to three orbitals involved (as is the case in most of the data) then a ballpark estimate of the confinement scale is given approximately by $2.4T$. It varies very slowly with truncation of the orbitals as seen in the ideal case. The Schottky peak corresponding to HF interaction results in a peak around $T = 40$ MeV, which results in an average splitting of about 90 MeV as given by potential models.

An analysis of the so-called exotic states in the charmonium sector seems to indicate that they are indeed unusual states due to the absence of the usual confinement peak, but exhibit a peak at a lower T, about 100 MeV, corresponding to a lower "exotic confinement" scale at ~240 MeV.

(ii) Our conclusions in the case of bottomonium states are similar to the charmonium states. The HF interaction is much weaker here as it should be if one uses the intuition from potential models. These states also exhibit the confinement peak at around 200 MeV. Interestingly, the so-called exotics again display a peak at about 100 MeV, similar to the exotics in the charmonium sector.

(iii) The analysis of open charm and open bottom states is more complicated but nevertheless we do get some insight into the scales involved.

Finally without going into details, we add a few comments on the light quark sector. The light quark sector is the most complicated since here the intuition from the potential models is not as clean as in the case of the heavy quark sector. Furthermore, the HF splitting is comparable to the confinement scale. This results in a single broad peak which may be due to a combination of confinement and HF splitting. Both in nonstrange and strange quark pseudoscalar bound states the confinement scale shifts to a much larger value due to the complication arising from the masses of the pion and K-meson. However, when $J \neq 0$ states are analyzed they display the confinement peak as witnessed in all other sectors. This buttresses the well-known problem with pions, that they are too light to be simple bound states of a quark and an antiquark [42]. This is also true, to a lesser extent, with the pseudoscalar K-mesons around 495 MeV.

While we have analyzed the data on meson spectra here, we may analyze the baryon spectra also from this perspective. In some ways this later analysis is likely to provide complimentary information further simplified by the fact that only quarks are involved unless the exotics are considered. This analysis is under way and will be published later [43].

ACKNOWLEDGMENTS

We thank R. K. Bhaduri for many suggestions and careful reading of the manuscript. The ideas outlined in the paper originated during the discussions in the HEP Journal Club. We thank all the members of JC for their helpful comments, especially Srihari Gopalakrishna, D. Indumathi, and Rahul Sinha.

[1] R. Aaij *et al.* (LHCb Collaboration), Phys. Rev. Lett. **115**, 072001 (2015).
[2] For a detailed review, see S. L. Olsen, Front. Phys. **10**, 121 (2015).
[3] For more detailed experimental references for all the exotic states, see [2] and the references therein.
[4] R. H. Dalitz, T. C. Wong, and G. Rajasekaran, Phys. Rev. **153**, 1617 (1967).
[5] R. Dalitz and S. Tuan, Ann. Phys. (N.Y.) **10**, 307 (1960).
[6] G. Rajasekaran, Phys. Rev. D **5**, 610 (1972).
[7] J. M. M. Hall, W. Kamleh, D. B. Leinweber, B. J. Menadue, B. J. Owen, A. W. Thomas, and R. D. Young, Phys. Rev. Lett. **114**, 132002 (2015).
[8] A. Esposito, A. L. Guerrieri, F. Piccinini, A. Pilloni, and A. D. Polosa, Int. J. Mod. Phys. A **30**, 1530002 (2015).
[9] R. K. Bhaduri, L. E. Cohler, and Y. Nogami, Phys. Rev. Lett. **44**, 1369 (1980).
[10] S. Godfrey and J. Napolitano, Rev. Mod. Phys. **71**, 1411 (1999).
[11] G. T. Bodwin, E. Braaten, E. Eichten, S. L. Olsen, T. K. Pedlar, and J. Russ, in *Community Summer Study 2013: Snowmass on the Mississippi (CSS2013) Minneapolis, 2013*, edited by N. A. Graf, M. E. Peskin, and J. L. Rosner (2013).
[12] N. Brambilla *et al.*, Eur. Phys. J. C **71**, 1534 (2011).
[13] S. Godfrey and S. L. Olsen, Annu. Rev. Nucl. Part. Sci. **58**, 51 (2008).
[14] R. K. Bhaduri and M. Dey, Phys. Lett. **125B**, 513 (1983).
[15] R. K. Bhaduri and W. van Dijk, Nucl. Phys. **A485**, 1 (1988).
[16] K. A. Olive *et al.* (Particle Data Group), Chin. Phys. C **38**, 090001 (2014).
[17] K. Abe *et al.* (Belle Collaboration), Phys. Rev. Lett. **98**, 082001 (2007).
[18] S. K. Choi *et al.* (Belle Collaboration), Phys. Rev. Lett. **91**, 262001 (2003); B. Aubert *et al.* (*BABAR* Collaboration), Phys. Rev. D **71**, 071103 (2005); D. Acosta *et al.* (CDF Collaboration), Phys. Rev. Lett. **93**, 072001 (2004); V. M. Abazov *et al.* (D0 Collaboration), Phys. Rev. Lett. **93**, 162002 (2004); S. Chatrchyan *et al.* (CMS Collaboration), J. High Energy Phys. 04 (2013) 154.
[19] R. Aaij *et al.* (LHCb Collaboration), Eur. Phys. J. C **72**, 1972 (2012).
[20] T. Aaltonen *et al.* (CDF Collaboration), Phys. Rev. Lett. **102**, 242002 (2009); S. Chatrchyan *et al.* (CMS Collaboration), Phys. Lett. B **734**, 261 (2014).
[21] M. Ablikim *et al.* (BESIII), Phys. Rev. Lett. **110**, 252001 (2013); Z. Q. Liu *et al.* (Belle Collaboration), Phys. Rev. Lett. **110**, 252002 (2013).
[22] P. Pakhlov *et al.* (Belle Collaboration), Phys. Rev. Lett. **100**, 202001 (2008).
[23] C. Z. Yuan *et al.* (Belle Collaboration), Phys. Rev. Lett. **99**, 182004 (2007).
[24] B. Aubert *et al.* (*BABAR* Collaboration), Phys. Rev. Lett. **95**, 142001 (2005); Q. He *et al.* (CLEO Collaboration), Phys. Rev. D **74**, 091104 (2006).
[25] X. L. Wang *et al.* (Belle Collaboration), Phys. Rev. Lett. **99**, 142002 (2007); B. Aubert *et al.* (*BABAR* Collaboration), Phys. Rev. Lett. **98**, 212001 (2007).
[26] S. K. Choi *et al.* (Belle Collaboration), Phys. Rev. Lett. **100**, 142001 (2008); R. Aaij *et al.* (LHCb Collaboration), Phys. Rev. Lett. **112**, 222002 (2014).
[27] First reference in [25].
[28] M. Ablikim *et al.* (BESIII Collaboration), Phys. Rev. Lett. **111**, 242001 (2013).
[29] R. Mizuk *et al.* (Belle Collaboration), Phys. Rev. D **78**, 072004 (2008); J. P. Lees *et al.* (*BABAR* Collaboration), Phys. Rev. D **85**, 052003 (2012).
[30] K. Chilikin *et al.* (Belle Collaboration), Phys. Rev. D **90**, 112009 (2014).
[31] G. Pakhlova *et al.* (Belle Collaboration), Phys. Rev. Lett. **101**, 172001 (2008).
[32] C.-Y. Wong, Phys. Rev. C **69**, 055202 (2004).
[33] M. B. Voloshin, Phys. Lett. B **604**, 69 (2004).
[34] E. S. Swanson, Phys. Lett. B **588**, 189 (2004).
[35] E. Braaten and M. Kusunoki, Phys. Rev. D **69**, 114012 (2004).
[36] S. Pakvasa and M. Suzuki, Phys. Lett. B **579**, 67 (2004).
[37] S. Chatrchyan *et al.* (CMS Collaboration), J. High Energy Phys. 04 (2013) 154.
[38] C. Bignamini, B. Grinstein, F. Piccinini, A. D. Polosa, and C. Sabelli, Phys. Rev. Lett. **103**, 162001 (2009).
[39] K. F. Chen *et al.* (Belle Collaboration), Phys. Rev. Lett. **100**, 112001 (2008).
[40] A. Bondar *et al.* (Belle Collaboration), Phys. Rev. Lett. **108**, 122001 (2012).
[41] P. Krokovny *et al.* (Belle Collaboration), Phys. Rev. D **88**, 052016 (2013).
[42] C. Adolph *et al.* (COMPASS Collaboration), Phys. Rev. Lett. **114**, 062002 (2015).
[43] A. Biswas, M. V. N. Murthy, and N. Sinha (to be published).